

Interactive comment on “Evaluation of the 15-year ROM SAF monthly mean GPS radio occultation climate data record” by Hans Gleisner et al.

Hans Gleisner et al.

hgl@dmi.dk

Received and published: 3 March 2020

Author’s reply to Referee Comment 2 (RC2)

(1) Note that Figure 8 is actually broken down into latitudes. The latitude-resolved results in Figure 8 are discussed in Section 5.1. It is true that the vertically averaged time-series in Figs. 9 and 10 are only provided as global averages. The idea is that Figure 8 provides a detailed view across height and latitude for a limited set of RO missions and for bending angle only, while Figs. 9 and 10 provide a more complete view across RO missions and also for dry temperature. We will consider adding a table showing latitude-resolved vertically- and time-averaged RO mission differences as suggested by the reviewer. The exact contents of that table will have to be decided

C1

after further considerations.

(2) The monthly mean data are provided on a 2D latitude-height grid. This is now mentioned up front in the Introduction: “. . . we present results from an evaluation of the ROM SAF monthly-mean climate data records (CDRs) provided on a two-dimensional latitude-height grid, . . .”

(3) The multi-center inter-comparisons (Ho et al, 2009; Steiner et al., 2013) primarily resulted in quantifications of the trend differences between processing centers for RO variables retrieved from CHAMP data. Those results gave a first view of the uncertainties in the trends to be expected caused by differences between processing centers. The RO mission differences presented here constitute an additional source of uncertainty for the trends of long-term time series of RO data. However, we have only presented the differences themselves. We have not described the consequences for the long-term trends. We will come back to this issue in a future study, and by then we will hopefully be able to compare our results with an extended study of multi-center differences including several RO missions.

(4) Yes, it is possible to first combine the data and then do sampling error correction. This is actually our preferred method for constructing long multi-mission data records. However, it does not avoid the need to do sampling error correction as a remedy for differences in the sampling characteristics between RO missions. Either way (first do sampling error correction then combine data sets, or first combine data sets and then do sampling error correction) it is necessary to do sampling error correction if we want to avoid spurious long-term variability in the combined time series as new satellite missions replace older ones.

(5) We have updated the first paragraph of Section 2.1 accordingly:

The ROM SAF CDR v1.0 includes data from four RO missions: CHAMP, GRACE, COSMIC, and Metop. The processing of data from the first three missions was based on low-level input data from UCAR, while the Metop data were processed with input

C2

data from EUMETSAT. In addition, we also processed Metop data using input data from the University Corporation for Atmospheric Research (UCAR), to allow for investigation of differences related to the low-level input data. The low-level input data consist of amplitude and excess phase data, together with positions and velocities for Global Positioning System (GPS) and low-Earth orbit (LEO) satellites. The input data versions are shown in Table 1. During the time period, COSMIC and GRACE experienced version updates, where the latter included a switch to zero-differencing in the generation of excess phases.

Concerning the question of whether there is quality control done on the low-level data, we know that EUMETSAT does it and it is actually taken into account in our own QC. Regarding UCAR data, we would assume there is a certain degree of low-level quality control and data rejection. However, it is difficult to find detailed documentation on that, and it is also a bit out of the scope of this article to go into such detail.

(6) We have added a new second paragraph to Section 3.2:

High noise levels and other errors may lead to occultations being rejected by the quality screening. Any errors in the retained bending angles may propagate further down the processing chain, since bending angles are the starting point for the retrieval of the other geophysical variables. In particular, bending angle data in the upper stratosphere is affected by residual ionospheric errors resulting in errors in refractivity and dry temperature lower down in the stratosphere.

(7) The jump that we see in the RO-ERA-I differences (Figure 5) in October 2009 is related to a bias shift in ERA-Interim. It is our understanding that this bias shift in ERA-Interim was caused by an update of the COSMIC data processing at UCAR, leading to a change in the data being assimilated by the ERA-Interim reanalysis system. The reference provided (Healy, 2013) states that the change in the operational processing of COSMIC data took place on October 12, 2009, which is consistent with what we see in our data records.

C3

(8) The inter-mission differences in the 4-8 km height range are actually larger for bending angle than for refractivity. The effect can also be seen in Figure 6 for time-averaged data. It is partly a matter of the vertical scale of the plots: the bending angle is plotted as a function of impact altitude while the refractivity is plotted versus altitude. The two vertical height variables can differ by up to 1-2 km near the surface. The downward propagation of information through the Abel transform also means that at a particular height (altitude or impact altitude) in the 4-8 km height range, less biased data from higher atmospheric layers contribute a larger fraction of the data for the refractivity compared to bending angle.

(9) We have now updated the text in Section 3.3 in order to provide somewhat more information:

Before processing the atmospheric profiles to gridded monthly-mean data, all profiles are checked against a set of quality criteria. The quality criteria include tests to identify occultations that a) do not provide any meaningful bending angles or only provide bending angles in a limited height range, b) have degraded bending angles indicated by increased noise in the L2 signal or by certain types of deviation from a bending-angle climatology, c) could be regarded as outliers as evidenced by comparison with ECMWF reanalysis data, or d) encounter problems in the 1D-Var processing. More detailed descriptions of the data quality screening are found in the series of validation reports available at the ROM SAF web site (http://www.romsaf.org/product_documents.php).

If an occultation does not pass one or several of the tests in a, b, or c, the bending angle, refractivity, and dry variables are marked as non-nominal. Otherwise, they are regarded as nominal and the refractivity profiles are passed on to the 1D-Var processing. The fraction of data rejected in the quality screening varies with time (Fig. 1). On average, around 10-20% of the occultations are rejected, although with large differences between the RO missions. Metop and GRACE show the highest throughput of data; almost no data are rejected by criterion a and about 5-10% are rejected by criteria b and c. COSMIC and CHAMP have roughly similar overall rejection rates. However,

C4

for COSMIC about 5-10% of data are rejected by criterion a, while for CHAMP that criterion removes about 15% or even more of the data.

(10) The purpose of the division into sub-bins is to compute a bin mean that as closely as possible approximate an area-weighted mean:

$$\bar{X} = \frac{1}{A} \int X dA \quad (1)$$

where X is a geophysical variable and A is the bin area. The main problem that is addressed by the weighting is non-uniform sampling of X across the bin. As stated in the text, we only consider the non-uniform distribution of observations in latitude. The division of the 5-degree latitude bins into two sub-bins can be regarded as a very coarse discretization of the above mentioned integral. During time periods with a lot of RO data, and for monthly bins, a finer discretization would be possible. However, we want to use the same binning across the whole time series, from CHAMP to COSMIC and Metop, and, hence, we chose two sub-bins for the 5-degree main bins.

(11) First a clarification: as stated in Section 3.6, by the “mean seasonal cycle” we mean the long-term average as a function of latitude, height, and season. For each latitude, height, and January month, we average across many years. Similarly for all February months, etc. This is what Eq. 10 expresses. Our “mean seasonal cycle” is a sum of the long-term means (i.e. means across all seasons) and the seasonal cycle on top of that long-term mean. We do not separate the two.

Let's say that we have two overlapping missions, A and B. Should we compute anomalies for A using data from A as reference, and anomalies for B using B data as reference, we wouldn't be able to detect constant biases between the missions. The same argument could be made even if we separate long-term means from the seasonal cycle: we wouldn't be able to detect differences in the seasonal cycle as measured by A and by B.

C5

In addition, assume that we generate long-term climatologies from several non-overlapping RO missions. If we construct the anomalies using mission-specific anomaly references, we would not only remove any biases (systematic errors) between the missions, but also true climatological time variations.

(12) In Section 4, we now mention that even though the magnitude of the RO-ERA-Interim difference suddenly decreased as a result of the start of assimilation of COSMIC data in 2006, the difference remains slightly negative in the 12-20 km height interval throughout the data record.

(13) In our input data we find differences between the EUMETSAT and UCAR LEO orbits with the right magnitude, and with a periodicity of one orbit, that potentially could explain the hemispheric differences that we observe (see Figure 1). The source, and the ultimate cause, of these orbital differences is still a matter of ongoing work. More detailed information can also be found in the series of validation reports available at http://www.romsaf.org/product_documents.php. It is, however, still premature and out of the scope of this paper to include a detailed description of what we believe is the cause of the differences.

(14) The purpose of the bullet list is to summarize our own observations of inter-mission biases as shown in Figure 8 (and to some extent Figure 9). In some bullets we also point out possible causal relations, a few of them well-known while other should be regarded as preliminary conclusions from the present study itself. We will add references to the first bullet (signal tracking issues) and the third bullet (Metop software upgrades).

(15) No, the Metop-COSMIC globally averaged differences that we see in Figure 9 would be very similar for Metop(UCAR) as for Metop(EUM). You can see this in Figure 8, by comparing the middle column (Metop(UCAR) minus COSMIC) with the right-most column (Metop(EUM) minus COSMIC). The dominating differences between Metop(UCAR) and Metop(EUM) are a large-scale hemispheric asymmetry (see the top panels in Figure 8) and some differences in the lower troposphere.

C6

(16) The Metop-COSMIC bias shift in 2013 can also be identified in Figure 8, where you also can see the latitude distribution of the shift. It is related to firmware upgrades in the Metop RO instruments described by the third bullet in Section 5.1.

(17) Mission acronyms are now spelled out in the Introduction.

(18) We have now expanded Section 2.2 somewhat, partly based on the comments of another reviewer. We also added a new reference (Healy and Thépaut, 2006) that provides a detailed description of the forward-modelling to refractivity and bending angle.

We used ERA-Interim reanalysis (Dee et al., 2011) data as a reference in the evaluation. To avoid the direct impact of the observed data on our comparison reference (RO data are assimilated by ERA-Interim), we used the reanalysis forecasts rather than analyses. ERA-Interim provides forecasts at three-hour intervals, initialized at 00 and 12 UTC. Hence, the shortest possible forecast time vary from 3 hours to 12 hours. For each RO event, a co-located vertical profile of model data was obtained by interpolation in the global forecast fields representing the atmospheric state at three-hour intervals (UTC 00, 03, ...) on a 1.0 x 1.0 latitude-longitude grid.

The vertical profiles of model data (pressure, temperature, and humidity as function of geopotential height) are forward-modelled to the set of geophysical variables used in this study. The model refractivity is calculated from the Smith-Weintraub equation, and the bending angles are obtained by an Abel integral over the refractivity profile assuming an exponential decay above the model top (Healy and Thépaut, 2006). Dry temperature profiles are computed from the model refractivities using the same method as for the observed profiles (see Section 3.1). This is followed by monthly averaging in latitude bins and interpolation onto an equidistant 200 meter height grid, using the methods described in Section 3.4.

(19) Section 5.2 now begin with: “*The RO mission differences have so far been described ...*”.

C7

(20) The notation “6-8 km” was used to indicate that this is not an exact altitude. We have now changed four occurrences of “6-8 km” in the manuscript to “8 km” (in Abstract and in Sections 1 and 5.1).

Interactive comment on Atmos. Meas. Tech. Discuss., doi:10.5194/amt-2019-417, 2019.

C8

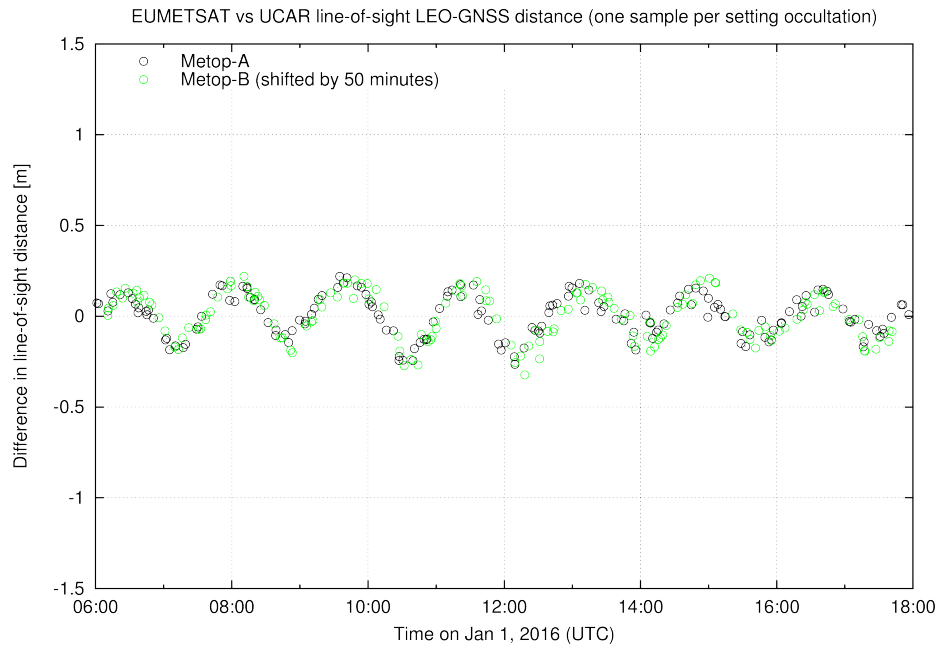


Fig. 1. Differences between Metop orbits from EUMETSAT and UCAR, as quantified by the differences in the Metop-GPS distances.